(9) Handy, C. T.; Rothrock, H. S. *J. Am. Chem. Soc.* **1958**, *80*, 5306–5308.
(10) Mayo, F. R.; Miller, A. A.; Russell, G. A. *J. Am. Chem. Soc.* **1958**, *80*, 2500.
(11) Klebanskii, A. L.; Sorokina, R. M. *Zh. Prikl. Khim.* **1962**, *35*, *12*, 2735–2740.
(12) Cordischi, D.; Lenzi, M.; Mele, A. *Trans. Faraday Soc.* **1964**, *60*, 503, 2047–2053.
(13) Caglioti, V.; Lenzi, M.; Mele, A. *Nature (London)* **1964**, *201*, 610–611.
(14) Gozzo, F.; Carraro, G. *Nature (London)* **1965**, *206*, 507–508.
(15) Ta-Hsun, Lu; Pao-Tung; Hsiao-Chiang, Chao. *Huaxue Xuebao* **1966**, *32*, 34–45.
(16) Craig, T. O.; Tyrall, E. *J. Polym. Sci., Part B* **1967**, *5*, 10, 955–957.
(17) Ivanchev, S. S.; Zherebin, Yu. L. *Dokl. Akad. Nauk. SSSR* **1973**, *208*, 3, 664–667.
(18) Tsvetkov, N. S.; Lukyanets, V. M.; Zhukovskii, V. Ya. *Tezisy Dokl.—Ukr. Resp. Konf. Fiz Khim., 12th* **1977**, 70–71.
(19) Bovey, F. A.; Kolthoff, I. M. *J. Am. Chem. Soc.* **1947**, *69*, 2143.
(20) Miller, A. A.; Mayo, F. R. *J. Am. Chem. Soc.* **1956**, *78*, 1017.
(21) Mayo, F. R.; Miller, A. A. *J. Am. Chem. Soc.* **1956**, *78*, 1023–1034.
(22) Russell, G. A.; Mayo, F. R. U.S. Patent 2 794 055, 1957.
(23) Mayo, F. R. *J. Am. Chem. Soc.* **1958**, *80*, 2465–2480.
(24) Van Sickle, D. E.; Mayo, F. R.; Arluck, R. M.; Syz, M. G. *J. Am. Chem. Soc.* **1967**, *89*, 967.
(25) Mayo, F. R.; Castelman, J. K.; Mill, T.; Silverstein, R. M.; Rodin, O. *J. Org. Chem.* **1974**, *39*, 889.
(26) Kishore, K. *J. Chem. Eng. Data* **1980**, *25*, 99.
(27) Mayo, F. R.; Cais, R. E. *Macromolecules* **1981**, *14*, 885–886.
(28) Kishore, K.; Ravindran, K.; Nagarajan, R. *J. Polym. Sci., Polym. Lett. Ed.* **1984**, *22*, 539–542.
(29) Kishore, K.; Mukundan, T. *Nature (London)* **1986**, *324*, 130.
(30) Galibei, V. I.; Arkhipova-Kalenchenko, E. G. *Zh. Org. Khim.* **1977**, *13*, 227–228.
(31) Chuchin, A. E.; Kallnova, I. Yu. *Otkrytiya, Izobret., Prom. Obraztsy, Tovarnye Znaki* **1976**, *53*, 21, 236.
(32) Budtov, V. P.; Ivanchev, S. S.; Balyaev, V. M.; Romanova, O. S.; Otradina, G. A. *Vysokomol. Soedin. Ser. A* **1976**, *18*, 2328.
(33) Barnes, C. E.; Elofson, R. M.; Jones, G. D. *J. Am. Chem. Soc.* **1950**, *72*, 210.
(34) Chang, P.; Tien, Yu. L. *Huaxue Xuebao* **1958**, *24*, 135.
(35) Mayo, F. R. *J. Am. Chem. Soc.* **1958**, *80*, 2493–2497.
(36) Kerber, R. *Makromol. Chem.* **1960**, *40*, 25.
(37) Kishore, K.; Ravindran, K. *J. Anal. Appl. Pyrolysis* **1983**, *5*, 363–370.
(38) Cais, R. E.; Bovey, F. A. *Macromolecules* **1977**, *10*, 169–178.
(39) Kissinger, H. E. *Anal. Chem.* **1957**, *29*, 1702.
(40) Mayo, F. R.; Miller, A. A. *J. Am. Chem. Soc.* **1956**, *78*, 1023.
(41) Kishore, K.; Ravindran, K. *Macromolecules* **1982**, *15*, 1638.
(42) Benson, S. W. *Thermochemical Kinetics*, 2nd ed.; Wiley: New York, 1976.
(43) Van Krevelen, D. W. *Properties of Polymers*, 2nd ed.; Elsevier: New York, 1976; p 451.
(44) Guthrie, J. P.; Kathleen, F. T. *Can. J. Chem.* **1983**, *61*, 602.
(45) Weast, R. C. Ed. *CRC Handbook of Chemistry and Physics*, 59th ed.; CRC Press: Cleveland, 1978.
(46) Karapetyants, M. Kh.; Karapetyants, M. L. *Thermodynamic Constants of Inorganic and Organic Compounds*; translated by J. Schmorak; Ann Arbor-Humphrey Science: Ann Arbor, MI, London, 1970.
(47) Deen, J. A., Ed. *Lange's Handbook of Chemistry*, 11th ed.; McGraw Hill: New York, 1973.
(48) Mark, H. F.; Gaylord, N. G. *Encycl. Polym. Sci. Technol.* **1970**, 13.
(49) Brandrup, J., Immergut, E. M., Eds. *Polymer Handbook*; Interscience: New York, 1975.
(50) Sawada, H. *Thermodynamics of Polymerization*; Marcel Dekker: New York, 1976; p 341.
(51) Roberts, J. D.; Caserio, M. C. *Modern Organic Chemistry*; W. A. Benjamin: New York, 1967.

Monte Carlo Calculations for Linear Chains and Star Polymers with Intramolecular Interactions. 4. Dimensions and Hydrodynamic Properties below the Θ State

Antonio Rey and Juan J. Freire*

Departamento de Quimica Fisica, Facultad de Ciencias Quimicas, Universidad Complutense, 28040 Madrid, Spain

José Garcia de la Torre

Departamento de Quimica Fisica, Facultad de Ciencias Quimicas y Matemáticas, Universidad de Murcia, 30001 Murcia, Spain. *Received January 20, 1987*

ABSTRACT: Calculations on the radius of gyration and hydrodynamic properties of linear and several types of uniform star polymers of different lengths (the latter properties obtained in a nonpreaveraged way) have been performed in order to reproduce solvent conditions below the unperturbed state (previous simulations in this region only cover the radius of gyration of linear chains). The model used for these calculations considers Gaussian distances between neighboring units and also a Lennard-Jones (LJ) potential to describe interactions between nonneighboring units. This model has been already used in previous work to study the Θ and good solvent regions by setting the appropiate values of the LJ energetic parameters. The results and their combinations in terms of ratios g, h, and g' of the properties of the star polymers to those of the linear chains and in terms of the hydrodynamic molecular parameters P, Φ, and β for each given chain are reported and discussed. The decrease of the contraction (or expansion) for chains with an increasing number of arms and the slower changes in the hydrodynamic properties with varying solvent power with respect to the changes in the radius of gyration are the main conclusions of the study.

Introduction

In previous work,[1-3] we have numerically investigated the solution properties of linear and starlike polymers described through a molecular model with intramolecular interactions by means of Monte Carlo conformational simulations. The model consists of $N + 1$ units whose intramolecular distances to their nearest neighbors follow a Gaussian distribution with root mean squared (rms) deviation, b, equivalent to the familiar statistical length of a Gaussian subchain. The nonneighboring units interact through an effective Lennard-Jones (LJ) potential

$$V_{ij} = 4\epsilon[(\sigma/r_{ij})^{12} - (\sigma/r_{ij})^{6}] \quad (1)$$

where r_{ij} is the distance between the interacting units i and

0024-9297/87/2220-2385$01.50/0

j. The rationale of this model was described in ref 1. The LJ reduced parameter ϵ/k_BT tries to mimic the balance of intramolecular and polymer–solvent interactions so that varying this parameter is equivalent to changing temperature–solvent conditions. The assignment of parameters has been performed according to our numerical results for the mean quadratic radius of gyration, $\langle S^2 \rangle$, of linear chains with different numbers of units.[1] Thus, the reduced steric parameter is set to the value $\sigma/b = 0.8$ which is adequate to reproduce a significant expansion of the chains in the high-temperature (or good solvent) region, employing a number of units small enough to be reasonably handled in the calculations. Also, the value $\epsilon/k_BT = 0.3$ yields the value $\nu = 0.5$ in the scaling law relationship[4]

$$\langle S^2 \rangle \propto N^{2\nu} \tag{2}$$

and, therefore, is assigned to the "unperturbed" or "Θ" conditions. (This definition of Θ conditions from eq 2 is not completely rigorous[4] and, moreover, recent experimental studies[5] show that the Θ state may vary with the topology in the case of short chains, though the differences vanish for longer chains. Then, our unperturbed state should be understood as the reference value $\epsilon/k_BT = 0.3$ for which one can reasonably expect an exponent value close to $\nu = 0.5$ in the long-chain limit.) In the same study of linear chains[1] we found $\nu = 0.6$ for $\epsilon/k_BT = 0.1$, and, therefore, we consider this value as representative of the good-solvent conditions.

With these assignments in mind we have already completed the study of the dimensions,[1,3] or $\langle S^2 \rangle$, and hydrodynamic properties,[2,3] namely, the translational friction coefficient, f_t, and the intrinsic viscosity, $[\eta]$, of linear and star chains (defined through the number of uniform arms, F) in both the unperturbed[1,2] and the good solvent[3] regions. Here, we report the Monte Carlo results corresponding to very poor solvent conditions, i.e., with $T < \Theta$. In this region a contraction of the polymer is expected due to the predominant intramolecular attractive forces. The dependence of the global properties of the model details are then enhanced and (as will be remarked in the discussion) one cannot expect to reproduce the real polymer behavior with quantitative accuracy. However, the differences in the contraction due to the topology of the chain or the specific property employed for its characterization can be revealed at least in a general way. A further motivation for our calculations is the lack, to the best of our knowledge, of previous simulations of either star chains or hydrodynamic properties in these solvent conditions.

Method and Results

The simulation methods to generate conformations according to their Boltzmann probabilities and following the Metropolis criterion were extensively described in our previous work[1] and will not be repeated here. We should only remark that the stochastic process used in the present calculations consists of changing the position of a single randomly selected unit per step, i.e., process b described in ref 1. (A different process in which we change a part of an arm per step is used for $T \geq \Theta$.) Once a conformation has been generated, we calculate $\langle S^2 \rangle$ (in numerical units relative to b^2) from the double-sum of quadratic distances between pairs of chain units. We calculate the dimensionless coefficients

$$f_t^* = f_t/6\pi\eta_0 b \tag{3}$$

$$[\eta]^* = [\eta]M/N_A b^3 \tag{4}$$

also as functions of the different unit positions. The calculation of hydrodynamic properties is performed assuming that each conformation can be considered as a rigid body.[6] We treat these rigid structures with an elaborate algorithm due to Garcia de la Torre and Bloomfield[7] within the frame of the Kirkwood–Riseman theory. This algorithm avoids orientational preaveraging and makes use of a modified Oseen tensor that describes properly the hydrodynamic interactions even when these interactions occur between overlapping units (overlapping of units is common in the studied temperature range because the local density of units is rather high). The reduced translational friction of each element is introduced by means of a dimensionless parameter h^*, proportional[2] to the translational friction coefficient of the units and inversely proportional to $\eta_0 b$, which is set to the value $h^* = 0.25$, very close to that of a Gaussian coil. We analyse the results for eight independent stochastic processes (or samples), each one initiated with a different seed number. For the calculation of dimensions we generate 250 000 conformations per sample. For the hydrodynamic properties (with distributions considerably narrower than those of $\langle S^2 \rangle$) we employ 3000–50 000 conformations to drive each stochastic process but calculate the properties of only a 10% randomly selected fraction of the sample.

In Table I we present the results obtained for $\langle S^2 \rangle$, f_t^*, and $[\eta]^*$ with the different choices of N and F and the values $\epsilon/k_BT = 0.4$ and 1.0. The variation of $\alpha^2 = \langle S^2 \rangle / \langle S^2 \rangle_\Theta$ with changing ϵ/k_BT for chains of $N + 1 = 37$ units and different functionalities is presented in Figure 1. (Results corresponding to $\epsilon/k_BT \leq 0.3$ previously reported are also included.) In Figures 2 and 3 we show the results obtained for the expansion coefficients α_f^2 and α_η^2 of linear

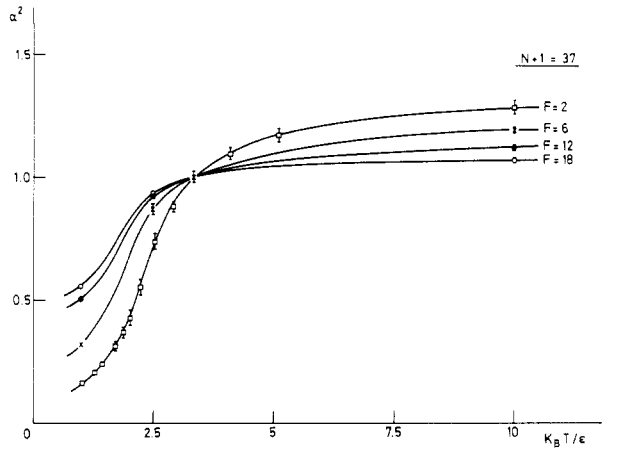

Figure 1. α^2 vs. k_BT/ϵ for chains of different functionalities with $N + 1 = 37$.

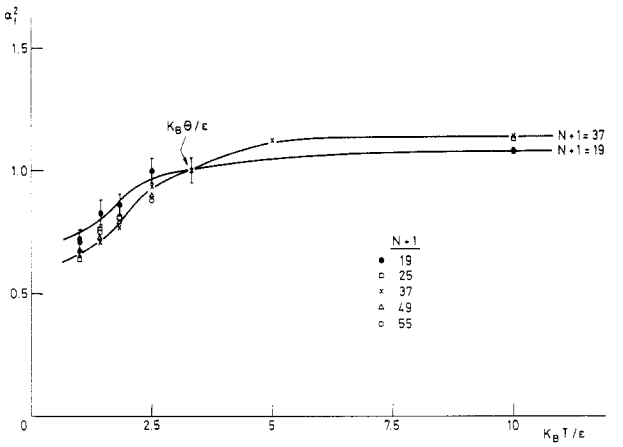

Figure 2. α_f^2 vs. k_BT/ϵ for linear chains of different lengths.

Table I
Results and Ratios g, h, and g' for Different Values of ϵ/k_BT, F, and N[a]

ϵ/k_BT	F	$N+1$	$\langle S^2\rangle$	f_t*	$[\eta]$*	g	h	g'
0.4	2	19	3.66 ± 0.04	1.37 ± 0.03	37 ± 5			
		25	4.68 ± 0.09	1.54 ± 0.02	48 ± 2			
		37	6.2 ± 0.2	1.94 ± 0.05	94 ± 10			
		49	7.5 ± 0.8	2.28 ± 0.06	150 ± 20			
		55	7.6 ± 0.4	2.43 ± 0.04	180 ± 10			
	6	19	2.142 ± 0.003	1.28 ± 0.03	25 ± 2	0.585 ± 0.007	0.93 ± 0.04	0.7 ± 0.1
		37	3.82 ± 0.03	1.89 ± 0.03	79 ± 5	0.62 ± 0.02	0.97 ± 0.04	0.8 ± 0.2
		49	4.72 ± 0.05	2.17 ± 0.04	115 ± 8	0.63 ± 0.07	0.95 ± 0.02	0.8 ± 0.2
		55	5.16 ± 0.08	2.31 ± 0.02	138 ± 4	0.68 ± 0.05	0.95 ± 0.02	0.76 ± 0.08
	12	25	1.978 ± 0.003	1.39 ± 0.03	29 ± 2	0.423 ± 0.009	0.90 ± 0.03	0.60 ± 0.07
		37	2.729 ± 0.008	1.71 ± 0.03	52 ± 3	0.44 ± 0.01	0.88 ± 0.04	0.55 ± 0.09
		49	3.42 ± 0.02	1.97 ± 0.03	80 ± 5	0.46 ± 0.05	0.87 ± 0.04	0.5 ± 0.1
	18	19	1.527 ± 0.001	1.18 ± 0.01	16.6 ± 0.5	0.42 ± 0.05	0.86 ± 0.03	0.45 ± 0.07
		37	2.302 ± 0.004	1.62 ± 0.01	44 ± 1	0.37 ± 0.01	0.84 ± 0.03	0.47 ± 0.07
		55	3.212 ± 0.007	1.99 ± 0.02	80 ± 3	0.42 ± 0.02	0.82 ± 0.02	0.44 ± 0.05
1.0	2	19	1.11 ± 0.01	1.16 ± 0.03	19 ± 4			
		25	1.188 ± 0.005	1.28 ± 0.03	24 ± 2			
		37	1.43 ± 0.02	1.63 ± 0.05	53 ± 4			
		49	1.66 ± 0.06	1.96 ± 0.05	95 ± 10			
		55	1.8 ± 0.1	2.18 ± 0.08	130 ± 20			
	6	19	1.176 ± 0.004	1.21 ± 0.01	20 ± 1	1.06 ± 0.01	1.04 ± 0.04	1.1 ± 0.3
		37	1.40 ± 0.01	1.77 ± 0.04	66 ± 6	0.98 ± 0.02	1.09 ± 0.06	1.2 ± 0.2
		49	1.63 ± 0.01	2.11 ± 0.02	106 ± 3	0.98 ± 0.04	1.08 ± 0.04	1.1 ± 0.2
		55	1.75 ± 0.02	2.15 ± 0.03	112 ± 6	0.97 ± 0.06	0.99 ± 0.05	0.8 ± 0.1
	12	25	1.176 ± 0.006	1.36 ± 0.03	27 ± 2	0.990 ± 0.009	1.17 ± 0.06	1.4 ± 0.4
		37	1.50 ± 0.01	1.67 ± 0.02	49 ± 2	1.05 ± 0.05	1.02 ± 0.04	0.9 ± 0.1
		49	1.60 ± 0.01	1.93 ± 0.03	76 ± 4	0.96 ± 0.04	0.98 ± 0.04	0.8 ± 0.2
	18	19	1.328 ± 0.002	1.17 ± 0.01	16.4 ± 0.5	1.2 ± 0.1	1.01 ± 0.03	0.9 ± 0.2
		37	1.367 ± 0.009	1.59 ± 0.02	40 ± 2	0.96 ± 0.02	0.98 ± 0.04	0.75 ± 0.09
		55	1.85 ± 0.02	1.99 ± 0.01	81 ± 2	1.03 ± 0.07	0.89 ± 0.05	0.61 ± 0.09

[a] Statistical errors obtained from the rms deviations are included.

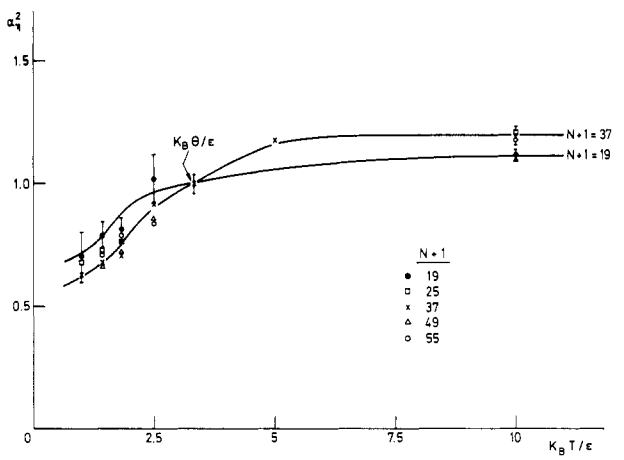

Figure 3. α_η^2 vs. k_BT/ϵ for linear chains of different lengths.

chains of several lengths at different values of ϵ/k_BT. Those coefficients are defined as

$$\alpha_f^2 = (f_t/(f_t)_\Theta)^2 \quad (5)$$

$$\alpha_\eta^2 = ([\eta]/[\eta]_\Theta)^{2/3} \quad (6)$$

and would be equivalent to α^2 if the proportionalities $f_t \propto \langle S^2\rangle^{1/2}$ and $[\eta] \propto \langle S^2\rangle^{3/2}$, established for long Gaussian chains, could be maintained in the whole range of temperatures. In Table I we also report the ratios of the properties of each given star chain to those corresponding to linear chains of the same number of units ($g = \langle S^2\rangle_b/\langle S^2\rangle_l$, $h = (f_t)_b/(f_t)_l$, and $g' = [\eta]_b/[\eta]_l$, where subscripts b and l refer to the branched and linear chain).

The results for a given chain can be combined in terms of useful molecular parameters (that would be independent of N if the proportionality between f_t, $[\eta]$, and $\langle S^2\rangle$ were obeyed):

$$P = f_t/6^{1/2}\eta_0\langle S^2\rangle^{1/2} \quad (7)$$

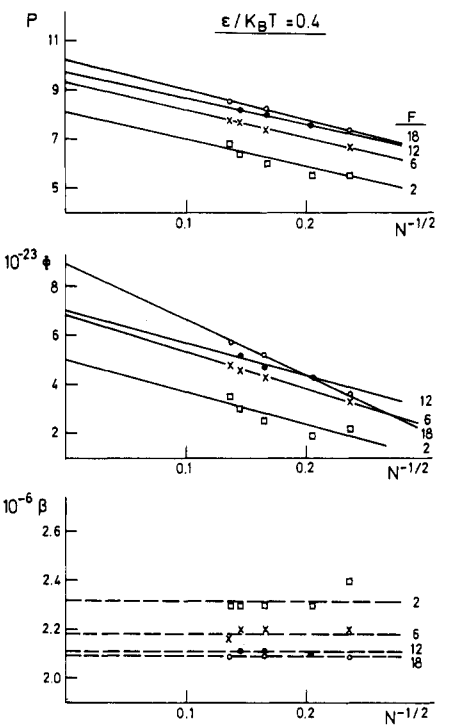

Figure 4. Parameters P, Φ, and β vs. $N^{-1/2}$ and extrapolations to $N^{-1/2} = 0$. $\epsilon/k_BT = 0.4$. Different functionalities.

which is simply related to the ratio of the rms radius of gyration to the Stokes law hydrodynamic radius, $\rho = 6^{1/2}\pi/P$,

$$\Phi = [\eta]M/6^{3/2}\langle S^2\rangle^{3/2} \quad (8)$$

and

$$\beta = (M[\eta]/100)^{1/3}\eta_0/f_t \quad (9)$$

Table II
Summary of Values Obtained through Extrapolation to the Long-Chain Limit[a]

ϵ/k_BT	F	g	h	g'	P	$10^{-23}\Phi$	$10^{-6}\beta$
Gaussian	2				6.2 ± 0.2	2.54 ± 0.08	2.28 ± 0.05
	6	0.444	0.86 ± 0.01	0.58 ± 0.02	7.8 ± 0.2	4.9 ± 0.2	2.18 ± 0.02
	12	0.236	0.75 ± 0.01	0.38 ± 0.03	9.2 ± 0.3	7.6 ± 0.8	2.16 ± 0.02
	18	0.160	0.66 ± 0.01	0.24 ± 0.03	9.3 ± 0.2	7.4 ± 0.9	2.10 ± 0.08
0.4	2				8.1 ± 0.6	5 ± 1	2.31 ± 0.04
	6	0.67 ± 0.03	0.950 ± 0.005*	0.75 ± 0.02*	9.3 ± 0.4	6.8 ± 0.7	2.18 ± 0.01
	12	0.52 ± 0.06	0.84 ± 0.08	0.4 ± 0.2	9.7 ± 0.8	7 ± 1	2.11 ± 0.01
	18	0.38 ± 0.01*	0.80 ± 0.03	0.450 ± 0.009*	10.2 ± 0.2	8.9 ± 0.3	2.095 ± 0.004
1.0	2				16 ± 1	29 ± 4	2.21 ± 0.01
	6	0.90 ± 0.04	1.05 ± 0.02*	1.0 ± 0.1	18.7 ± 0.4	41 ± 2	2.168 ± 0.007
	12	0.99 ± 0.01*	0.8 ± 0.1	0.4 ± 0.4	16.2 ± 0.8	28 ± 3	2.116 ± 0.006
	18	0.75 ± 0.04	0.89 ± 0.05	0.5 ± 0.2	16.2 ± 0.2	25 ± 1	2.097 ± 0.005
global fit					16.7 ± 0.2	29.0 ± 0.6	2.13 ± 0.01
rigid sphere		1	1	1	9.93	9.23	2.12

[a] The Gaussian results were reported previously;[10] (*) arithmetic means (see text); statistical errors included.

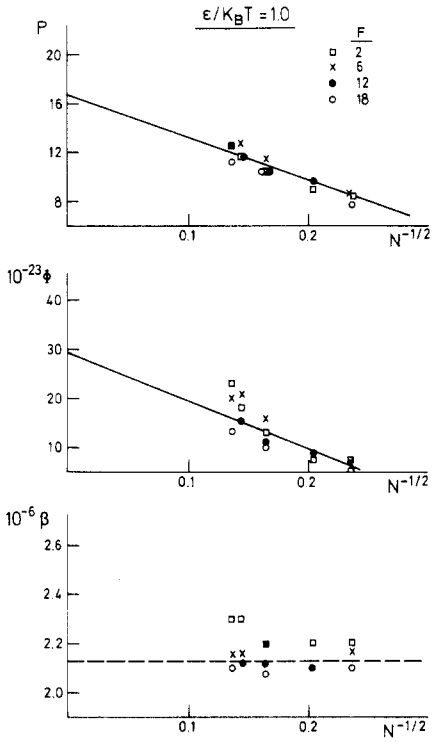

Figure 5. As in Figure 4 but with $\epsilon/k_BT = 1.0$.

The values of these parameters obtained with $\epsilon/k_BT = 0.4$ and $\epsilon/k_BT = 1.0$ are represented vs. $N^{-1/2}$ in Figures 4 and 5 for chains of different functionalities.

We have performed tentative extrapolations to the high molecular weight (or high N) limit of all these combined results. The extrapolations were carried out through linear regression analysis of P and Φ vs. $N^{-1/2}$, based in the predictions of simpler Kirkwood–Riseman treatments[6] (see Figures 4 and 5) and a similar analysis of g, h, and g' vs. N^{-1}, according to the detailed analysis of results corresponding to Gaussian stars[9] (see Tables I and II). In some of the latter extrapolations we have not found a reasonable correlation in the results so that in these cases we prefer to estimate the extrapolated ratios as simple arithmetic means over the results obtained for chains with different units (the cases are denoted by an asterisk in Table II). The extrapolated values of β in Figures 4 and 5 are also estimated as arithmetic means (β does not depend much on N).

In Table II we sumarize the extrapolated results for the different choices of F and ϵ/k_BT. For $\epsilon/k_BT = 1.0$ we also show the extrapolated value obtained in a regression analysis of all the values of P and Φ corresponding to chains of different functionalities (the parameters practically are insensitive to F for such poor temperature–solvent conditions). In fact, these fittings are the ones represented in Figure 5. For the sake of comparison we also include in Table II values corresponding to the Gaussian chain[10] and a rigid sphere. Simulation values corresponding to the unperturbed and good solvent regions are given in ref 1–3.

It should be remarked that our model is sensitive to finite size effects that can somewhat distort the extrapolation procedures, especially those corresponding to P and Φ. These numerical difficulties have been extensively discussed in our previous work.[1-3] At any rate, we believe that the extrapolated results, though only aproximated, are accurate enough to give a qualitative description of the behavior of the model in the long-chain limit and to reach the general conclussions that will be stated in the next section.

Discussion

The variation of α^2 with varying ϵ/k_BT for linear chains with $N + 1 = 37$ and different values of the functionality, shown in Figure 1, can be discussed in terms of its comparison with the curves corresponding to linear chains of different lengths (Figure 1 of ref 1).

In Figure 1 and successive similar figures of this work, the lines are smooth curves and some statistical error bars have been introduced for illustrative purposes. It can be observed that the star molecules exhibit a more modest change of dimensions from the poor to the good solvent conditions, the globular form associated with poor conditions being reached sooner as the number of arms increases. This is a consequence of the more compact average shape of star chains in the region above $T \geq \Theta$ imposed by the topology of the chain. In general, a higher value of F for a given value of N implies shorter arms and therefore, a smaller expansion capability. Thus, one can perform a simple comparison of the ratio between the expansion coefficients of a star and a linear chain of the same number of units, $\alpha_s^2/\alpha_l^2 = g/g_\Theta$, in different solvent conditions. For $T \ll \Theta$, $g = 1$ since the distribution of monomers should be uniform inside the globule and, then, it does not depend on the chain topology. Since $g_\Theta < 1$ for any star chain, it is clear that $\alpha_s^2 > \alpha_l^2$. In the good solvent region, recent experimental data[11,12] for linear and star samples obey the general pattern $g < g_\Theta$, which is clearly observed for the higher functionality $F = 18$, in agreement also with the previous lattice simulations of Kolinski and Sikorski[13] in the good and Θ regions. Though all these facts seem to confirm our conclusions, we should mention that they are in contradiction with recent theories

of excluded volume in star polymers[14,15] that predict a sharper variation of α^2 with varying temperatures as F increases, apparently overestimating the expansion effects in star molecules (this controversy between theory and simulation data is also pointed out in ref 13, where some previous theoretical and numerical works are also invoked). We hope that future experimental work on star polymers in the whole solvent power range will clarify this point. We should also remark that the values of g, h, and g' obtained for unperturbed Gaussian chains (i.e., using a model without intramolecular interactions or excluded volume) are in very close agreement with the values obtained in the very good solvent limit.[3,16,17] As the solvent power decreases it seems that the steric effects due to the central core of the star chains cannot be eliminated in simple extrapolation of simulation results to the long-chain limit, and they are also manifested in experimental data of higher molecular weight samples, these effects being more noticeable for higher functionalities. Of course, in the globular state all the different types of chains adopt a global form similar to that of the central core.

The results for g, h, and g' contained in Table I and their tentative extrapolations to the long-chain limit (Table II) can be easily understood according to the arguments given in the preceding paragraph. As we approach to the globular state, the differences in size between linear and star chains tend to vanish and the different ratios tend to increase up to unity. In fact, for the lowest temperature, $\epsilon/k_BT = 1.0$, case in which the uncertainties in our simulations are higher due to a severe reduction of the conformational space, we find that some of our results are accidently greater than this limit. In all the cases with $T < \Theta$ we can observe a considerable departure of the extrapolated ratios from the values corresponding to the good solvent region.

Figures 2 and 3 show that the transition curves for α_f^2 and α_η^2 are significantly less abrupt than the α^2 curve. Thus, we cannot claim to have reached the constant hydrodynamic radius which would manifest the globular state through the hydrodynamic properties. Slower variations of these properties with varying solvent power in comparison with the change in dimensions have been recently found in experimental measurements.[18] Also, this behavior has been predicted through the use of simple double-sum hydrodynamic treatments in the frame of the renormalization group theory.[19] The effect can be explained as an increase of the partial draining of the chain in better solvents caused by the lowest monomer density inside the coil. As a consequence, the effective hydrodynamic radius is shrunk so that its increase due to the chain expansion is partially compensated. (For the highest functionalities both effects practically cancel out and we cannot observe much change in the hydrodynamic radius in the whole temperature range.) Then the measurements of the radius of gyration are more suitable to describe a transition from very poor to good solvent conditions than the less sensitive, though experimentally simpler, measurements of hydrodynamic properties.

The extrapolated values of molecular parameters contained in Table II deserve also a detailed discussion. As to parameter β, we should comment that it is not very sensitive to temperature or solvent condition changes. Since its dependence on N is very modest, we can confidently propose the relationship $\alpha_\eta \approx \alpha_f$. On the other hand, the standard preaveraged hydrodynamic treatment should lead to spurious variations of β with varying solvent conditions. The standard result for a Gaussian chain is about a 15% greater than the nonpreaveraged value[2] and we believe that preaveraging is less reliable as the compactness of the molecular structure increases, i.e., in our case as the solvent quality decreases. This belief is supported by our earlier work on star polymers (preaveraged results are less accurate as F increases[10]) and rigid structures[20] (orientational preaverage introduces more error in the more compact forms). Then the argument that expansion coefficients are insensitive to preaveraging[19] should be taken with caution. A slightly higher dependence of β on the topology of the chain is noticed, though the parameter can be safely set within the range $\beta = (2.1\text{–}2.3) \times 10^6$ for all the chains in any solvent condition. This result can be helpful to relate diffusion (or sedimentation) and viscosity experiments with estimations of molecular weights.

The results obtained for P and Φ seem to be more sensitive to finite size effects and model details and, as a consequence, are less realistic. It can be observed that for these low temperatures P and Φ do not depend much on the number of arms. For $\epsilon/k_BT = 1.0$ the results for chains with the same number of units and different functionalities are very close. For $\epsilon/k_BT = 0.4$ the differences in the extrapolated results obtained from linear fittings and contained in Table II may be too high, since the curvatures shown by the different patterns of points in Figure 4 indicate closer real intercept values. The tendency to obtain higher values for smaller temperatures is clearly manifested and corresponds to the slower decrease of the hydrodynamic properties in comparison with the radius of gyration, according to the arguments exposed above. Experimental data (see ref 18 and Figure 2 of ref 19) support this conclusion. However, it is surprising that some of our results for P and Φ are well above those corresponding to a rigid sphere. This result can be expected if the chain behaves as an impenetrable sphere with a higher density of monomers in its central part. Such a model can be realistic in the region between the Θ and the globular state. In fact, the experimental data of a globule–coil transition followed by both radius of gyration and hydrodynamic radius measurements[18] show values of the ratio between both properties, $\rho = 0.74$, below the rigid sphere limit $\rho = 0.77$. Then, P should surpass the corresponding limit. Nevertheless, once a globular state composed of a compact arrangement of many units is reached, the rigid sphere limit should be obtained for any property. This is not the case for our model with $\epsilon/k_BT = 1.0$ because we have a few finite size spheres stuck together in a compact form that should show an irregular external surface. For this form P and Φ are above the sphere limit and, therefore, we cannot reproduce the globular state. In order to describe properly the region below the Θ point with a model, we will need to have a suficiently high number of units of volume much smaller than that of the globule, which would be outside our computational capability. Even so, we cannot be sure that a single reduced parameter ϵ/k_BT can reproduce the whole change of conditions, since ϵ represents an averaged balance between polymer units and solvent that may be temperature dependent. The steric parameter σ/b should also be smaller in the very poor solvent region, since the theoretical units can be chosen so that they are short enough to be absent of excluded volume effect in the good region, but it is not clear whether they may suffer a significant contraction below the Θ state.

In any case, the results reported here in the very poor solvent region are useful to discern the general features that can be correctly predicted by a manageable model with intramolecular interactions. Namely, we can show the constancy, increase, or decrease of properties, parameters, or ratios with varying temperature and even describe

qualitatively some subtle effects as the increase of P and Φ beyond the sphere limits. We can also perform a useful comparison of the transition curves that can be expected for different types of chains or properties. However, we cannot give a good quantitative description of the change of the properties with temperature in the form of scale laws or obtain the assymptotic values corresponding to the globular state. Of course, these type of results were not obtained in previous simulations for dimensions of linear chains with similar two-parameter intramolecular models.[21,22] In summary, we conclude that simple models can describe tendencies but not detailed dependencies in the $T < \Theta$ region. Given this situation, future simulation work should be directed not only to improving the calculation efficiency through more efficient algorithms but also to studying alternative models applicable to both the globular and the expanded coil states with similar adequacy.

Acknowledgment. This work was supported in part by a Grant from the Comision Asesora de Investigacion Cientifica y Tecnica (Grant 1409/82). A.R. acknowledges the award of the Enrique Moles fellowship (1984–1986).

References and Notes

(1) Freire, J. J.; Pla, J.; Rey, A.; Prats, R. *Macromolecules* **1986**, *19*, 452.
(2) Freire, J. J.; Rey, A.; Garcia de la Torre, J. *Macromolecules* **1986**, *19*, 457.
(3) Rey, A.; Freire, J. J.; Garcia de la Torre, J. *Macromolecules* **1987**, *20*, 342.
(4) de Gennes, P.-G. *Scaling Concepts in Polymer Physics*; Cornell University: Ithaca, NY, 1979.
(5) Bauer, B. J.; Hadjichristidis, N.; Fetters, L. J.; Roovers, J. E. L. *J. Am. Chem. Soc.* **1980**, *102*, 2410.
(6) Zimm, B. H. *Macromolecules* **1980**, *13*, 592.
(7) Garcia de la Torre, J.; Bloomfield, V. *Q. Rev. Biophys.* **1981**, *14*, 81.
(8) Garcia de la Torre, J.; Jiménez, A.; Freire, J. J. *Macromolecules* **1982**, *15*, 148.
(9) Prats, R.; Pla, J.; Freire, J. J. *Macromolecules* **1983**, *16*, 1701.
(10) Freire, J. J.; Prats, R.; Pla, J.; Garcia de la Torre, J. *Macromolecules* **1984**, *17*, 1815.
(11) Roovers, J.; Hadjichristidis, N.; Fetters, L. J. *Macromolecules* **1983**, *16*, 214.
(12) Huber, K.; Burchard, W.; Fetters, L. J. *Macromolecules* **1984**, *17*, 541.
(13) Kolinski, A.; Sikorski, A. *J. Polym. Sci., Polym. Chem. Ed.* **1982**, *20*, 3147.
(14) Miyake, A.; Freed, K. F. *Macromolecules* **1983**, *16*, 1228.
(15) Vlahos, C. H.; Kosmas, M. K. *Polymer* **1984**, *25*, 1607.
(16) Zimm, B. H. *Macromolecules* **1984**, *17*, 2441.
(17) Whittington, S. G.; Lipson, J. E. G.; Wilkinson, M. K.; Gaunt, D. S. *Macromolecules* **1986**, *19*, 1241.
(18) Sun, S. T.; Nishio, I.; Swislow, G.; Tanaka, T. *J. Chem. Phys.* **1980**, *73*, 5971.
(19) Wang, S.-Q.; Douglas, J. F.; Freed, K. *Macromolecules* **1985**, *18*, 2464.
(20) Garcia de la Torre, J.; López, M. C.; Tirado, M. M.; Freire, J. J. *Macromolecules* **1983**, *16*, 1221.
(21) Baumgärtner, A. *J. Chem. Phys.* **1980**, *72*, 871.
(22) Webman, I.; Lebowitz, J. L.; Kalos, M. H. *Macromolecules* **1981**, *14*, 1495.

Water Dynamics in Polyelectrolyte Solutions from Deuterium and Oxygen-17 Nuclear Magnetic Relaxation

J. R. C. van der Maarel, D. Lankhorst, J. de Bleijser, and J. C. Leyte*

Department of Physical and Macromolecular Chemistry, Gorlaeus Laboratories, University of Leiden, 2300 RA Leiden, The Netherlands. *Received February 24, 1987*

ABSTRACT: Longitudinal relaxation rates of D and ^{17}O were obtained in a concentration series of poly(acrylic acid) and poly(styrenesulfonic acid) solutions with various counterions. The effects of the degree of neutralization and excess simple electrolyte on the water dynamics have been investigated. From these data conclusions are reached about the range of the polyion–solvent dynamical perturbation. The dynamical behavior of water molecules is changed significantly as shown by the correlation times. The symmetry of the motion is discussed by comparison of D and ^{17}O relaxation.

I. Introduction

A multinuclear NMR investigation of water dynamics in low molecular weight electrolyte solutions was reported recently.[1] Mulder et al. reported a study of the anisotropic behavior of the solvent in poly(methacrylic acid) (PMA) solutions.[2] In the present contribution, results of D and ^{17}O NMR in poly(acrylic acid) (PAA) and poly(styrenesulfonic acid) (PSS) solutions are reported. In the interpretation of the nuclear relaxation of counterions in solutions of charged macromolecules the influence of the perturbed solvent dynamics is unknown. Apart from the intrinsic interest of the solvent behavior this is an additional motivation for the present investigation.

Although many proton relaxation studies of water dynamics in various solutions have been reported, an unambiguous interpretation is difficult. The proton longitudinal relaxation is governed by H–H dipolar interactions. The intra- and intermolecular contributions to the proton relaxation are of the same order of magnitude. As a consequence, a determination of the intramolecular contribution is very sensitive to the correctness of the estimation of the intermolecular part. However, both the D and ^{17}O nuclei relax by the quadrupolar interaction mechanism, which is dynamically an intramolecularly determined process, although the coupling constants may depend on the intermolecular interactions. Hence, the NMR spin–lattice relaxation time values are sensitive to the single molecular reorientational motion. Especially, because the principal directions of the interaction tensors of ^{17}O and D do not coincide, the symmetry of the motion may be investigated.[3]

Due to the possibly high linear charge density on polyions, in polyelectrolyte solutions the oppositely charged counterions may be strongly attracted by the charged chain. A useful description of the resulting distribution of counterions around the polyion is the Oosawa–Manning model.[4,5] The linear charge density on the polyion is described by the charge density parameter, ξ, ξ being the ratio of the electrostatic energy between neighboring charges on the chain to the thermal energy

$$\xi = e^2/4\pi\epsilon_0\epsilon AkT \quad (1)$$

Here, A denotes the distance between neighboring charged beads on the chain and the other symbols have their usual

0024-9297/87/2220-2390$01.50/0